Journal of Medicinal Chemistry

Drug Annotation

pubs.acs.org/jmc

Discovery and Early Clinical Development of 2-{6-[2-(3,5-Dichloro-4-pyridyl)acetyl]-2,3-dimethoxyphenoxy}-*N*-propylacetamide (LEO 29102), a Soft-Drug Inhibitor of Phosphodiesterase 4 for Topical Treatment of Atopic Dermatitis

Jakob Felding, Morten D. Sørensen, Tina D. Poulsen,[†] Jens Larsen, Christina Andersson,[‡] Pia Refer, Karen Engell, Lotte G. Ladefoged, Thorsten Thormann, Anne Marie Vinggaard,[§] Pontus Hegardt, Anders Søhoel, and Simon Feldbæk Nielsen*

New Product Discovery and Global Development, LEO Pharma A/S, Industriparken 55, 2750 Ballerup, Denmark

ABSTRACT: Development of orally available phosphodiesterase 4 (PDE4) inhibitors as anti-inflammatory drugs has been going on for decades. However, only roflumilast has received FDA approval. One key challenge has been the low therapeutic window observed in the clinic for PDE4 inhibitors, primarily due to PDE4 mediated side effects. Here we describe our approach to circumvent this issue by applying a soft-drug concept in the design of a topically acting PDE4 inhibitor for treatment of dermatological diseases. We used a fast follower approach, starting from piclamilast. In particular, simultaneous introduction of 2′-alkoxy substituents and changing an amide to a keto linker proved to be beneficial when designing potential soft-drug candidates. This effort culminated in identification of LEO 29102 (**20**), a potent, selective, and soft-drug PDE4 inhibitor with properties suitable for patient-friendly formulations giving efficient drug delivery to the skin. Compound **20** has reached phase 2 and demonstrated clinically relevant efficacy in the treatment of atopic dermatitis.

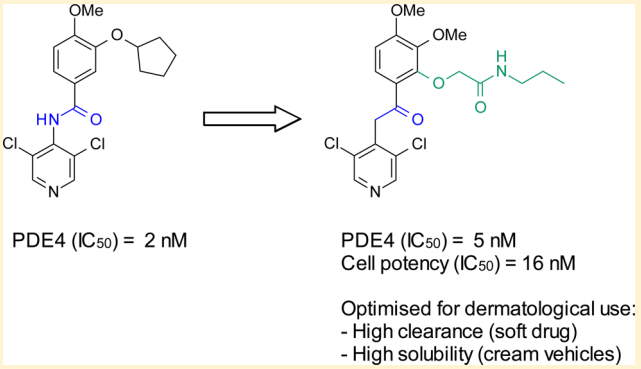

INTRODUCTION

Atopic dermatitis (AD) is the most common childhood skin disease and shows an increased prevalence in Western European countries and North America.[1,2] It is usually present during early infancy and childhood but can also start in adulthood and affects up to 20% of children and 3% of adults. The disease is a relapsing chronic inflammatory skin disease often associated with hyper-reactivity to environmental triggers and is characterized by eczematous skin plaques and intense itch (pruritus). The pruritus has a major impact on the quality of sleep and is associated with profound negative effects on the quality of life for AD patients and their family unit.[3] Furthermore, AD is believed to represent the initial step of the "atopic march", in which AD can develop into systemic diseases like asthma and allergic rhinitis.[4] Topical corticosteroids are still the mainstream therapy in the treatment of AD, but topical calcineurin inhibitors have also brought significant clinical benefit to AD patients.[5] However, new steroid-free anti-inflammatory agents that could provide a safe and effective long-term treatment for patients with AD would add significantly to the treatment options for this complex disease.

Phosphodiesterases (PDEs) belong to a family of 11 different isoenzymes that catalyze the hydrolysis of the two secondary signal messengers cyclic adenosine monophosphate (cAMP) and cyclic guanosine monophosphate (cGMP).[6] PDEs are classified accordingly into three groups: those that are (i) specific to cAMP and (ii) specific to cGMP and (iii) those that act on both cAMP and cGMP. Phosphodiesterase 4 (PDE4) enzymes belong to the first group, as they only participate in the regulation of cAMP levels. When PDE4 is inhibited, the resultant elevation of intracellular cAMP levels leads to an activation of specific protein phosphorylation cascades, which

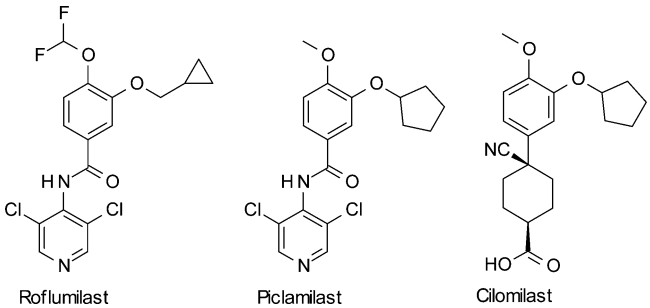

Figure 1. Selected PDE4 inhibitors in clinical trial at the outset of this program.[17]

Received: March 11, 2014

dx.doi.org/10.1021/jm500378a | *J. Med. Chem.* XXXX, XXX, XXX–XXX

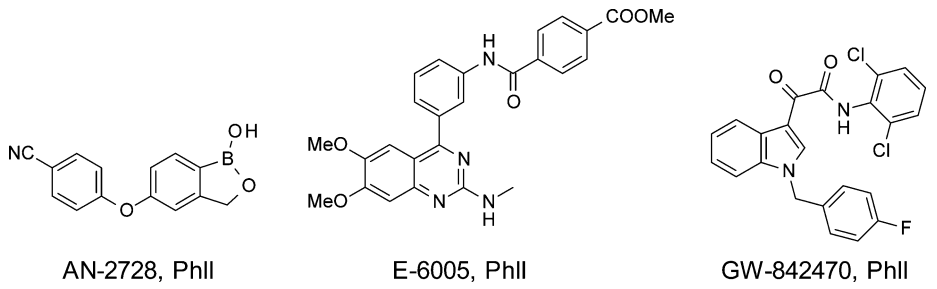

Figure 2. Structures of the most advanced PDE4 inhibitors for topical treatment of AD.[17]

Scheme 1. Synthesis Route for Variations in the 2′-O Position Exemplified by the Synthesis of 20[a]

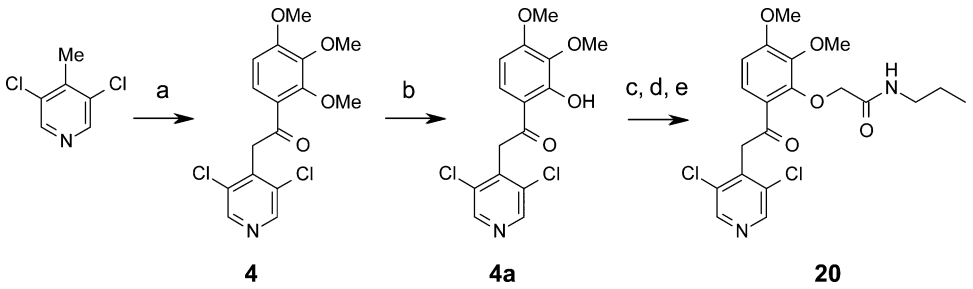

[a]Reagents and conditions: (a) methyl 2,3,4-trimethoxybenzoate, LiHMDS, THF, 0 °C (65%); (b) 1 M BCl_3 (74%); (c) ethyl bromoacetate, K_2CO_3 (78%); (d) LiOH, H_2O, MeOH (92%); (e) propylamine, HATU, DIPEA, DMF.

elicit a variety of functional responses in the inflammatory cells such as suppression of TNFα production. Four subtypes of PDE4 have been identified (PDE4A–PDE4D) that are encoded by four distinct genes.

Of these, PDE4A, -B, and -D are primarily found in inflammatory and immune cells, including T cells, B cells, macrophages, monocytes, neutrophils, and eosinophils.[7] Development of PDE4 inhibitors as a novel anti-inflammatory therapy has been ongoing for several decades with asthma and chronic obstructive pulmonary disease (COPD) as the primary indications. However, although a large number of PDE4 inhibitors have been evaluated in the clinic, roflumilast (Figure 1) is currently the only approved PDE4 inhibitor. A primary problem with PDE4 as a drug target is the narrow therapeutic window of PDE4 inhibitors, owing to the on-target gastrointestinal adverse effects (primarily nausea and emesis), which severely limits the dose that can be given. Indeed, for many oral PDE4 inhibitors in the clinic it is likely that the maximum tolerated dose is subtherapeutic.[8]

Although the vast majority of PDE4 inhibitors in the clinic are aiming for oral dosing, a small number of PDE4 inhibitors in late stage clinical testing are aiming for topical treatment of skin diseases (see Figure 2).

On the basis of the potential of PDE4 inhibition as a novel anti-inflammatory mechanism in the treatment of AD, we decided to embark on developing a soft-drug PDE4 inhibitor for topical treatment of AD. The soft drug concept is based on a rapid metabolic inactivation by loss of PDE4 activity in the resultant metabolites. Combining a soft-drug approach with topical application was chosen to limit the systemic exposure of the topically acting drug and thereby increase the therapeutic window. In this article, we describe the discovery and early development of the potent and selective soft-drug PDE4 inhibitor **20**,[16] which is being evaluated in phase 2 clinical trials for topical treatment of atopic dermatitis. We review the medicinal chemistry strategy, structure–activity relationships, and binding interaction to PDE4. We also discuss the preformulation characterization from a topical perspective, preclinical emetic potential, and initial clinical data.

MEDICINAL CHEMISTRY STRATEGY

Several compounds were in clinical development at the outset of the project (see Figure 1) and piclamilast caught our attention, as it was being developed for asthma, which could be considered a pseudotopical route of administration.[9] In addition, piclamilast contains two structural features with proven benefits for PDE4 inhibitors: (i) the diether catechol scaffold, which is a well described isostere of adenosine to mimic the nucleotide part of cAMP, and (ii) the 2,6-dichloropyridine moiety which represents a key motif for the high selectivity toward PDE4 and is also present in roflumilast. Importantly, the very low aqueous solubility of piclamilast, which could be advantageous for an inhaled product, was considered limiting for development of a dermatological product and the physicochemical profile of piclamilast needed to be optimized for our purpose. Taken together, a fast follower approach starting from piclamilast was seen as an attractive medicinal chemistry strategy to be able to rapidly progress the project.

Chemistry. 3′5-Dichloropyridine based derivatives, with a keto linker to connect the catechol moiety, were synthesized starting from **4**. The synthesis route for variations in the 2′-O position is exemplified with the structure of **20** in Scheme 1. Compound **4** was obtained by adding LiHMDS to a mixture of 3,5-dichloro-4-methylpyridine and methyl 2,3,4-trimethoxybenzoate in THF. When the benzylic anion of 3,5-dichloro-4-methylpyridine forms, it reacts in situ with the methyl ester group of methyl 2,3,4-trimethoxybenzoate to provide the desired keto linker in **4**. Derivative **3** was prepared under the same conditions but using methyl 3,4-dimethoxybenzoate in place of methyl 2,3,4-trimethoxybenzoate (not shown).

dx.doi.org/10.1021/jm500378a | J. Med. Chem. XXXX, XXX, XXX–XXX

A selective 2′-demethylation of **4** was achieved by treatment with BCl_3 to provide **4a**. The free 2′-OH phenol group of **4a** was alkylated with a variety of alkyl halides under basic conditions (K_2CO_3) to provide derivatives **8**−**11** and **22**. For compound **20** methyl bromoacetate was used as the alkylating reagent and the formed methyl ester was subsequently hydrolyzed using LiOH in a mixture of MeOH−water to provide derivative **14**. The free carboxylic acid of **14** was converted to a range of amide derivatives using a HATU-mediated amide coupling (derivatives **15**−**20**). When propylamine was used in the final amide coupling, **20** was obtained.

An alternative synthesis route was used for variations in the 3′-O position as exemplified for the synthesis of derivative **7** in Scheme 2. When **4** was treated with HI in glacial acetic acid at 80 °C, the 2′,3′-bis-demethylated intermediate **4b** was obtained.

Scheme 2. Synthesis Route for Variations in the 3′-O Position Exemplified by the Synthesis of 7[a]

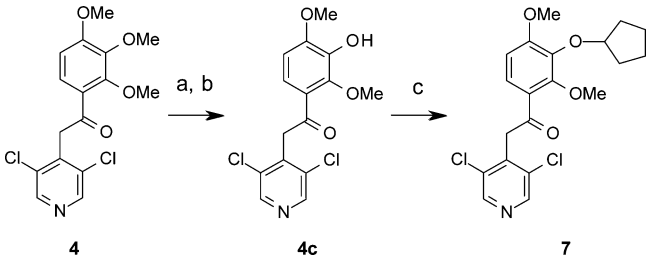

[a]Reagents and conditions: (a) HI on AcOH, 80 °C (81%); (b) 1 equiv of MeI, K_2CO_3, DMF (27%); (c) cyclopentyl bromide, K_2CO_3.

Upon treatment of **4b** with 1 equiv of methyl iodide under basic conditions (K_2CO_3) the 2′,4′-dimethylated intermediate (**4c**) could be isolated, although in a modest yield (27%). Alkylation of the free 3′-OH phenol group of **4c** with different alkyl halides under basic conditions (K_2CO_3) provided derivatives **5**−**7**. When cyclopentyl bromide was used in the final alkylation step, derivative **7** was obtained.

MEDICINAL CHEMISTRY STRATEGY: IDENTIFICATION OF SCAFFOLD

We initially focused on identifying a non-amide linker to connect the diether catechol and 2,6-dichloropyridine moieties, as we believed the secondary amide in piclamilast was negatively influencing the solubility of the compound because of the possible formation of a hydrogen bond network.

In the initial screening cascade we used inhibition of PDE4 (enzymatic assay) and inhibition of TNFα production in human inflammatory cells (cellular assay) as the two main drivers for our compound design. In addition, the most critical part of our optimization was to identify a suitable region in the molecule to introduce a soft spot, allowing a fast hepatic metabolism to metabolites with reduced activity. The 3′ and 4′ positions in the piclamilast series have been extensively explored,[9] whereas the 2′-position has, to the best of our knowledge, not been investigated. Our work started by exploring the effect of introducing a methoxy group in the 2′-position of **1**. Compound **1** was chosen as a model system for piclamilast and displayed reasonable potency toward PDE4D (see Table 1). However, the additional 2′-OMe substituent in **2** proved detrimental to the potency (see Table 1). On the basis of the conformation of piclamilast when bound

Table 1. Impact of Linker and 2′-Substituents on Enzymatic Potency (PDE4D) and Inhibition of TNFα Release from Human Blood Mononuclear Cells Stimulated with Lipopolysaccharide

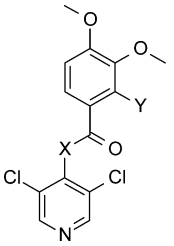

compd	X	Y	PDE4D IC_{50}[a] (nM)	TNFα IC_{50}[b] (nM)	QM energy[c] (kcal/mol)
1	NH	H	17	19	0.3
2	NH	OCH_3	3790	>5000	6.0
3	CH_2	H	13	11	0.5 (enol)
					0.0 (keto)
4	CH_2	OCH_3	110	436	0.0 (enol)
					2.8 (keto)

[a]Mean standard deviation is ±37%. [b]Mean standard deviation is ±60%. [c]Relative energy of the conformation similar to the bioactive conformation of piclamilast estimated by QM calculations.

to PDE4[10] (Figure 3A) where the amide carbonyl is orientated toward the 2′-position, we speculated that the lower potency of **2** compared to **1** is due to an unfavorable intramolecular interaction in the bioactive conformation between the 2′-O and the carbonyl of the amide linker.

We were however gratified to see that the corresponding two-atom keto linker had a very different profile. The 2′-unsubstituted amide and keto analogues were equipotent against PDE4D (**1** vs **3**), and 2′-OMe substitution only resulted in a 10-fold loss of potency when having the keto linker (**3** vs **4**) compared to a 200-fold loss for the amide linker (**1** vs **2**). A possible explanation could be that the two-atom keto linker, in the tautomeric enol form, has the possibility of forming an intramolecular H-bond to the 2′-O in the bioactive conformation. To further investigate this hypothesis, we performed a force field based coordinate scan and QM energy calculations. Both analyses supported a lower energy penalty for the bioactive conformation of an enol linker (and in fact also a keto linker) compared to the amide linker (Figure 3B, Table 1).

SAR of Substituents in the 2′- and 3′-Position. Encouraged by the promising PDE4D data as well as the inhibition of TNFα production in human inflammatory cells by derivative **4**, we sought to optimize potency by positioning the 3′-alkoxy group in the well-known lipophilic pocket of the enzyme to gain potency. However, this strategy was not very successful, as increasing the size of the 3′-alkoxy group beyond 3′-ethoxy provided less potent compounds (see Table 2). Apparently, the positioning of the 3′-alkoxy group is negatively influenced by the 2′-substituent and increasing the size to cyclopentyl (**7**, similar to piclamilast) totally eliminated activity.

At this point we obtained a crystal structure of an ethylisoxazole analogue of piclamilast (Figure 4A) which showed that the extended aromatic 3′-substituent of this derivative was involved in favorable hydrophobic interactions not observed for piclamilast. On the basis of this observation, we hypothesized that extended hydrophobic 2′-alkoxy substituents would have the potential to reach the ethylisoxazole pocket (Figure 4B). In addition to the hydrophobic interactions

dx.doi.org/10.1021/jm500378a | J. Med. Chem. XXXX, XXX, XXX−XXX

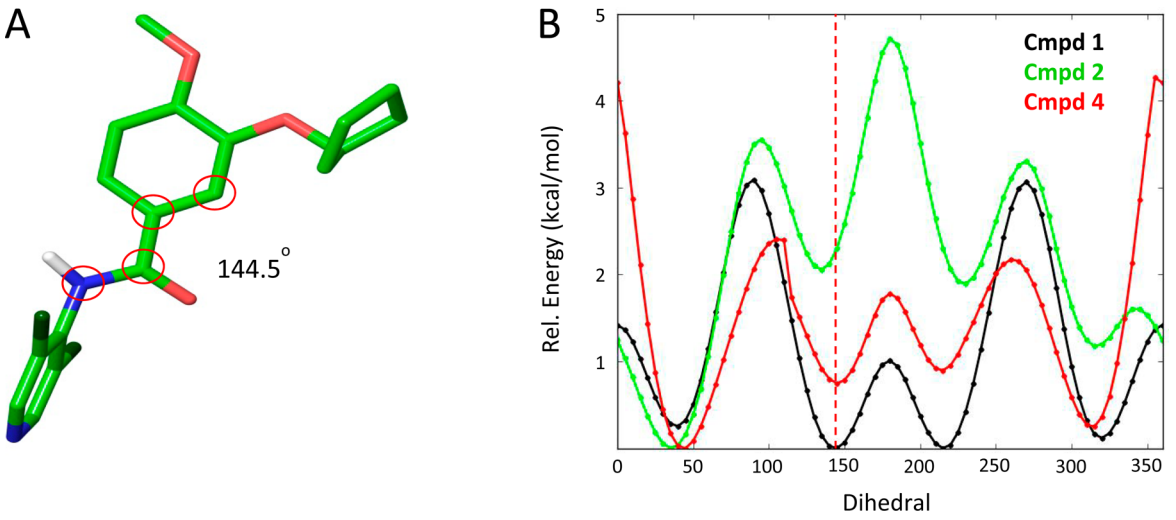

Figure 3. (A) Conformation of piclamilast taken from the crystal structure with PDE4 (1XM4). The dihedral C2−C1−C−N was measured after a MM energy minimization. (B) Plot of the relative (with respect to the global minimum energy) MM conformational energy obtained from a scan of the corresponding dihedral in compounds **1**, **2**, and **4** (enol form). The piclamilast "bioactive" dihedral is indicated by the dotted line. (The figures were made using Maestro; Schrödinger, LLC, New York, NY, 2013.)

Table 2. Impact of Varying 3′-Substituents on Enzymatic Potency (PDE4D) and Inhibition of TNFα Release from Human Blood Mononuclear Cells Stimulated with Lipopolysaccharide

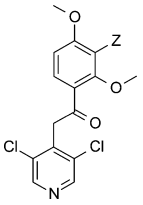

Compound	Z	PDE4D IC_{50}[a] nM	TNFα IC_{50}[b] nM
5		81	259
6	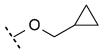	212	564
7		2010	9470

[a]Mean standard deviation is ±7%. [b]Mean standard deviation is ±55%.

observed for the ethylisoxazole group, it was also noteworthy that the terminal ethyl part extended toward the solvent accessible region (not shown).

We were pleased to find that 2′-*O*-benzyl substitution is allowed and in particular that 2′-*O*-phenethyl and 2′-*O*-phenylpropyl substitution brings sufficient potency to the compounds (**8**−**10**) albeit at the expense of increased lipophilicity (AlogP for **4** and **9** is 3.4 and 5.3, respectively) . The binding model of **9** suggested that the para position of the phenethyl would be solvent accessible and potentially could accommodate polar substituents. Accordingly, we introduced several substituents like hydroxy, amide, and even carboxylic acid (**11**−**13**) and found that hydrophilic para substitution is widely allowed in the 2′-*O*-phenethyl series. This was, however, quite unfortunate from a soft-drug perspective as the metabolism primarily occurs on the new phenyl ring, and these metabolites often proved highly active (e.g., the primary metabolite of **9** is the hydroxylation product **11**).

Reexamining the docking model suggested that charged groups positioned close to the core scaffold might be detrimental to the PDE4 activity because of the hydrophobic environment formed by Phe414, Met431, Phe446, and Ile450. As expected, compound **14** containing a short carboxylic acid substituent was inactive. Consequently, we prepared a range of amide analogues that potentially could be cleaved in the liver to **14**. Analogues containing a secondary amide moiety were all highly potent (**15**, **16**, **18**−**20**), whereas further substituting the amide moiety led to a drop in potency (**16** vs **17**).

To obtain further insight into the SAR of the amide series, we obtained a crystal structure of **15** complexed with PDE4D (Figure 5). Surprisingly, the crystal structure revealed that the binding mode of **15** is quite different from the docking model proposed for **9**. The 2′-substituent folds back in a conformation stabilized by an intramolecular H-bond between the 2′-amide NH and the linker oxygen, strongly suggesting that **15** binds in the keto form. Furthermore, there is a stabilizing hydrophobic collapse of the terminal aryl groups. Even more surprising was the observation (data not shown) of visible electron density for a C-terminal helix which made several interactions with **15**, most notably a H-bond with the side chain of Gln507 while the terminal benzyl forms π-stacking interactions with Phe506 and hydrophobic interactions with Leu510 (electron density for these residues could not be observed in the crystal structure with **9**). The crystal structure also readily explains the decrease in potency observed for **17** where an intramolecular H-bond cannot be formed.

As seen from Table 3, several compounds had satisfactory cellular potency and were rapidly metabolized by human liver microsomes. Next step was to identify the major metabolites and validate the metabolic inactivation (by loss of PDE4 activity), which is a prerequisite for a true soft-drug profile of the parent compound. The metabolism of **15** is shown in Figure 6, the primary metabolite being the inactive compound **14** together with minor amounts of two active metabolites (**21** and **22**). A similar pattern was observed for other amides including **20**.

dx.doi.org/10.1021/jm500378a | J. Med. Chem. XXXX, XXX, XXX−XXX

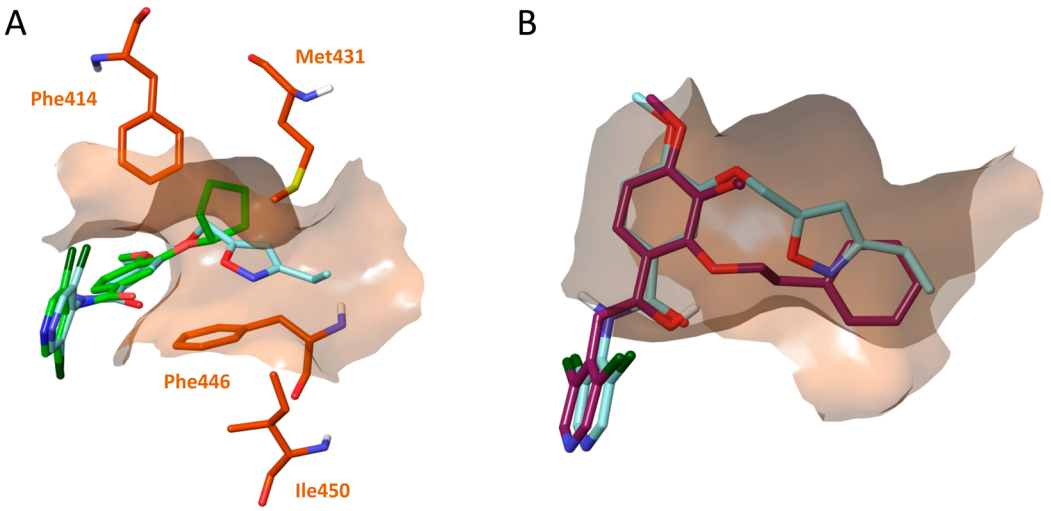

Figure 4. (A) Overlay of piclamilast (1XM4) and an ethylisoxazole analog in the PDE4 binding site. Residues involved in hydrophobic interactions with the ethylisoxazole substituent are shown. The crystal structure of the ethylisoxazole analogue complexed with PDE4D was solved to 2.2 Å. (B) Docking model of the enol form of **9** overlaid with the ethylisoxazole analogue. (The figures were made using Maestro; Schrödinger, LLC, New York, NY, 2013).

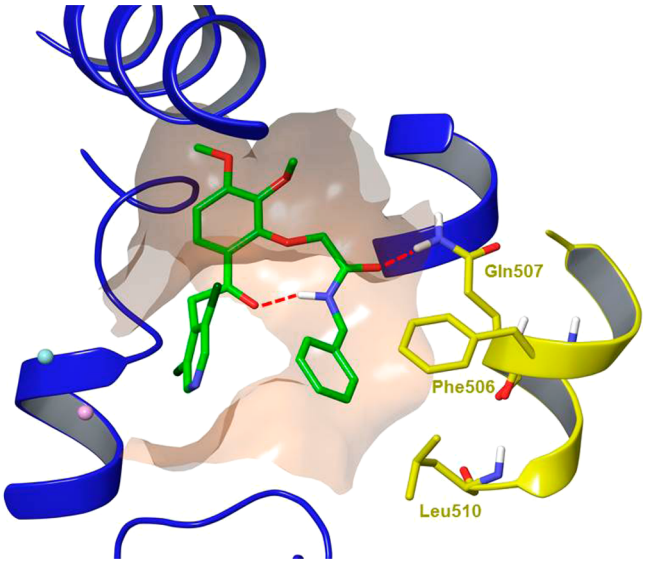

Figure 5. Crystal structure of compound **15** complexed with PDE4D solved to 2.5 Å. The additional C-terminal helix (residues 503−510) is shown in yellow highlighting the interactions with Phe506, Gln507, and Leu510. Residue numbering as in 1XM4. (The figure was made using Maestro; Schrödinger, LLC, New York, NY, 2013).

Four amides (**15**, **18**, **19**, and **20**) were selected for further profiling based on the above data and promising in vivo efficacy data. The compounds were tested in a topical allergic contact dermatitis model in mouse, consistently showing high level of efficacy after dermal dosing. Compound **20** demonstrated a dose dependent inhibition of TNFα in the tissue: 33%, 91%, and 100% inhibition at 0.001, 0.01, and 0.1 mg, respectively. In comparison betamethasone 17-valerate (0.003 mg) showed a 75% inhibition of TNFα.

PROFILING OF PRECANDIDATES

The four compounds (**15**, **18**, **19**, and **20**) were extensively profiled. The compounds and their main metabolites were profiled against 10 other human phosphodiesterases, showing them to be highly selective toward PDE4 (e.g., compound **20** and the main metabolite **14** showed less than 10% inhibition of PDE1−PDE11 at 1 μM, PDE6 not tested).

Likewise a "lead profile screen" against 68 primary molecular targets was performed, showing only PDE4 inhibition.[11] Genotoxicity was evaluated using the GreenScreen HC genotoxicity assay.[12] Unfortunately, **18** showed indications of in vitro genotoxicity at very high concentrations in the GreenScreen assay, and **18** was therefore deselected. Furthermore, compound **19** had, through metabolic demethylation, a potential to form **18** and was accordingly deselected as well (even though no genotoxicity was observed with **19**). On the basis of these findings, only compounds **15** and **20** were profiled further.

Final selection criteria were physicochemical properties suitable for the properties of topical formulations and a significantly improved emetic profile in vivo compared to other PDE4 inhibitors.

PREFORMULATION CHARACTERIZATION

The possibility for making an optimal dermal formulation is closely related to the solubility of the compound in solvents relevant for topical delivery and to the physical and chemical attributes of the compound related to the ability to penetrate the skin on its own. Since the release of the compound from the formulations is related to the diffusion of the compound from the vehicle to the skin, the maximum delivery from the vehicle is obtained with a compound dissolved in the vehicle close to saturation or supersaturated, resulting in a maximal thermodynamic drive. If it is not possible to dissolve the compound in any of the vehicle components, the compound needs to be suspended in the vehicle and dissolution rate and particle size will become determining steps for the drug release.

Assuming almost equal potency of **15** and **20**, we aimed for a concentration of compound in the final cream formulation of 0.25% (correlating to ~2000 μg/mL). To assess the potential for developing topical formulations, solubility in various relevant vehicles were determined. As seen in Table 4, the probability of dissolving the compound in the lipid part of the vehicle is highest for compound **20** which can be dissolved in different lipophilic solvents (e.g., MCT). Thus, formulating a

dx.doi.org/10.1021/jm500378a | J. Med. Chem. XXXX, XXX, XXX−XXX

Table 3. SAR of Substitution in the 2′-Position: Impact on Enzymatic Potency (PDE4D), Inhibition of TNFα Release from Human Blood Mononuclear Cells Stimulated with Lipopolysaccharide and Human Metabolic Degradation in Liver Microsomes (Expressed as Extraction Ratio, E_h)

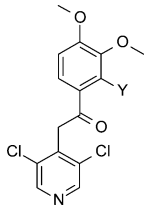

Compound	Y	PDE4D IC_{50}[a] nM	TNFα IC_{50}[b] nM	E_h
8	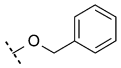	63	159	ND
9	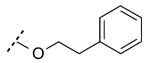	15	26	>91%
10	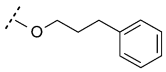	45	230	>91%
11	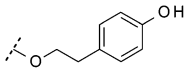	8	30	>91%
12	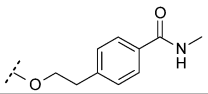	11	12	>91%
13	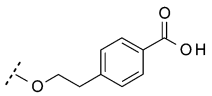	17	135	91%
14	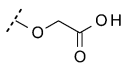	3760	>10000	<33%
15	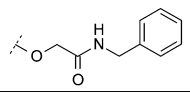	3	12	>91%
16	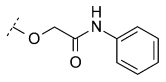	1	4	>91%
17	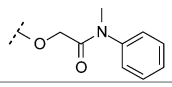	61	113	>91%
18	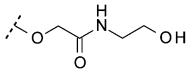	17	22	45%
19	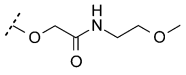	13	17	>91%
20	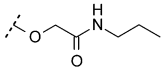	5	16	>91%
21	Pyridine N-oxide of **15**	5	11	72%
22	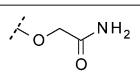	20	55	46%

[a]Mean standard deviation is ±36%. [b]Mean standard deviation is ±52%.

range of different prototypes of creams should be possible for this compound. In addition a formulation with **20** dissolved in the water phase is possible if propylene glycol is used as cosolvent. Compound **15** is less soluble, and a suspension

dx.doi.org/10.1021/jm500378a | J. Med. Chem. XXXX, XXX, XXX−XXX

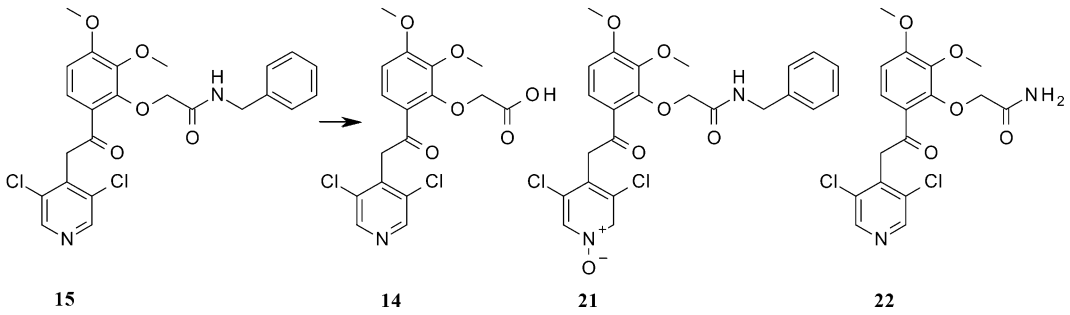

Figure 6. Hepatic metabolism of **15** in rat.

Table 4. Preformulation Data: Solubility in Vehicles Relevant for Topical Formulation

Compd	aqueous,[a,f] pH 7.4, μg/mL	20% HPCD,[b,e] μg/mL	MCT,[c,f] μg/mL	PG,[d,f] μg/mL	PG–H_2O,[f] 25:75, μg/mL	PG–H_2O,[f] 50:50, μg/mL	PG–H_2O,[f] 75:25, μg/mL
piclamilast	1	190	2000	3300			
15		57	580	990	2	20	230
20	14	220	6700	24000	135	1300	5600

[a]Phosphate buffer, 0.067 M, pH 7.4. [b]Hydroxypropyl-β-cyclodextrin in water. [c]mMedium chain triglyceride. [d]Propylene glycol. [e]The solubility was determined by shaking the compound in the vehicle for 1 h at room temperature. After centrifugation the concentration of compound in the supernatant was determined by HPLC. [f]The solubility was determined by shaking the compound in the vehicle for 24 h at room temperature. After centrifugation the concentration of compound in the supernatant was determined by HPLC.

cream would most likely be the outcome. Consequently compound **20** was selected for the final assessment of emetic risk.

EMESIS EVALUATION

The emetic potential of compound **20** was evaluated after iv dosing to ferrets. Although the PK profile of compound **20** may differ between ferrets and man, compound **20** showed comparable inhibition of human and ferret PDE4 enzyme. The animals were observed for a period of 2 h, and any emetic episode and/or associated prodromic signs (indications of nausea) were recorded. Compound **20** was very well tolerated up to the maximum feasible dose (1 mg/kg) with no emesis and no signs of nausea observed (Figure 7). As a comparison, cipamfylline (selective PDE4 inhibitor, evaluated topically in phase 2)[13] resulted in clear signals of emesis at 100 times lower doses (0.01 mg/kg).

Compound **20** was selected for further development based on the superior formulation properties and lack of emesis.

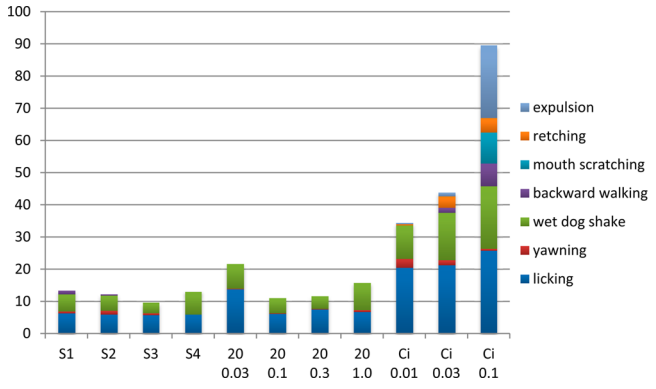

Figure 7. Cumulative emetic profile (number of episodes) of vehicle (S1–S4), compound **20** (0.03–1.0 mg/kg), and cipamfylline (Ci) (0.01–0.1 mg/kg) after iv dosing to ferrets.

EARLY CLINICAL DEVELOPMENT OF 20

The first study in man was a safety, tolerability, and pharmacokinetic study of single ascending and multiple cutaneous doses of **20** (2.5 mg/g cream).[14] A topical product for atopic dermatitis is likely to be used on large skin areas, and the clinical development must reflect that. Dose escalation was therefore performed by increasing the treated body surface area (BSA) up to 53% of BSA. Promising safety results were obtained, and no cases of emesis were observed in the study. The systemic PK profile supported the soft-drug concept obtaining very low systemic levels of active compound even if treated at a large body surface area (see Table 5).

Table 5. Geometric Mean C_{max} and AUC_{0-48h} after Singles Doses of 20–2.5 mg/g Cream to Healthy Subjects (n = 6 in each group) at Different BSA with Constant Amount of Cream per cm^2 [a]

	BSA dosed (%)			
	7	14	30	53
C_{max} (ng/mL)	0.279	0.754	2.39	5.07
AUC_{0-48h} (ng·h/mL)	5.45	14.9	49.2	100

[a]C_{max} and AUC values increased more than proportional to the dose (BSA), and an 8-fold increase in dose resulted in C_{max} and AUC values.

Subsequently **20** entered into a 4-week (phase 2) proof-of-concept and dose finding study, investigating treatment efficacy after dermal application of **20** cream, **20** cream vehicle, and Elidel cream.[15] The results were encouraging, and **20** entered into substantial clinical testing.

CONCLUSION

We have described the medicinal chemistry that resulted in the discovery of **20** (LEO 29102), which is a potent and highly selective PDE4 inhibitor with promising pharmaceutical properties that are suitable for effective topical delivery. The compound can be synthesized in a few simple synthetic steps, which is major advantage from a cost-of-goods perspective,

dx.doi.org/10.1021/jm500378a | J. Med. Chem. XXXX, XXX, XXX–XXX

since treatment of large body surfaces requires large amount of formulation to be applied (i.e., relatively large amount of compound) in a disease where treatment options are fairly low priced.

The applied soft-drug concept eliminated the PDE4 driven systemic side effects in both preclinical models and in the clinical setting. Furthermore, the clinical efficacy of **20** was clearly demonstrated in atopic dermatitis patients and further clinical studies were initiated.

EXPERIMENTAL SECTION

^{1}H nuclear magnetic resonance (NMR) spectra were usually recorded at 300 MHz. Chemical shift values (δ, in ppm) are quoted in the specified solvent relative to internal tetramethylsilane (δ = 0.00) or chloroform (δ = 7.25) or deuteriochloroform (δ = 76.81 for ^{13}C NMR) standards. The value of a multiplet, either defined (doublet (d), triplet (t), quartet (q)) or not (m) at the approximate midpoint is given unless a range is quoted. bs indicates a broad singlet. The organic solvents used were usually anhydrous. Chromatography was performed on Merck silica gel 60 (0.040−0.063 mm). Preparative HPLC/MS was performed on a Dionex APS-system with two Shimadzu PP150 preparative pumps and a Thermo MSQ Plus mass spectrometer with the following parameters: column, Waters XTerra C-18, 150 mm × 19 mm, 5 μm; solvent system, A = water (0.1% formic acid) and B = acetonitrile (0.1% formic acid); flow rate = 18 mL/min; method (10 min), linear gradient method going from 10% B to 100% B in 6 min and staying at 100% B for another 2 min. The fractions were collected based on ion traces of relevant ions and PDA signal (240−400 nm). All compounds were analyzed by UPLC−MS. High resolution chromatography was performed using the Waters Acquity UPLC and a 2.1 mm × 50 mm C18 RP column (1.8 μm particles). The mobile phases consisted of 0.1% formic acid in an aqueous 10 mM ammonium acetate solution for buffer A and 0.1% formic acid in acetonitrile for buffer B. A standard binary gradient was used for the reverse phase chromatography. All compounds had an estimated UV purity of >95% by UPLC−MS.

General Protocol for Preparation of 1 and 2. To a solution of an alkoxybenzoic acid (3 mmol) in toluene (10 mL) was added $SOCl_2$ (1 mL), and the reaction mixture was heated to 100 °C for 6 h. The reaction mixture was cooled to room temperature and evaporated. The alkoxybenzoyl chloride was redissolved in toluene (10 mL), evaporated, and then dissolved in THF (10 mL). 4-Amino-3,5-dichloropyridine (6 mmol) in THF (10 mL) was treated with NaH (6 mmol) for 3 h at room temperature followed by dropwise addition of the alkoxybenzoyl chloride solution (prepared above). After 4 h at room temperature the reaction was quenched with saturated NaCl (100 mL). The organic products were extracted with EtOAc (2 × 50 mL). The combined organic phases were dried over Na_2SO_4, evaporated in vacuo, and purified by flash chromatography using a gradient of EtOAc in heptane as eluent.

***N*-(3,5-Dichloro-4-pyridyl)-3,4-dimethoxybenzamide (1).** UPLC−MS (ESI+) *m*/*z* 327.03 (MH$^+$). ^{1}H NMR (300 MHz, DMSO-d_6) δ 10.43 (s, 1H), 8.74 (s, 2H), 7.68 (dd, *J* = 8.4, 2.1 Hz, 1H), 7.57 (d, *J* = 2.1 Hz, 1H), 7.12 (d, *J* = 8.4 Hz, 1H), 3.85 (s, 3H), 3.84 (s, 3H). Alkoxybenzoic acid: 3,4-dimethoxybenzoic acid.

***N*-(3,5-Dichloro-4-pyridyl)-2,3,4-trimethoxybenzamide (2).** UPLC−MS (ESI+) *m*/*z* 357.04 (MH$^+$). ^{1}H NMR (300 MHz, DMSO-d_6) δ 10.14 (s, 1H), 8.72 (s, 2H), 7.59 (d, *J* = 8.9 Hz, 1H), 6.99 (d, *J* = 8.9 Hz, 1H), 3.98 (s, 3H), 3.88 (s, 3H), 3.81 (s, 3H). Alkoxybenzoic acid: 2,3,4-trimethoxybenzoic acid.

2-(3,5-Dichloropyridin-4-yl)-1-(3,4-dimethoxyphenyl)-ethanone (3). Methyl 3,4-dimethoxybenzoate (98 mg, 0.5 mmol) and 3,5-dichloro-4-methylpyridine (105 mg, 0.65 mmol) was dissolved in dry THF (2 mL). The mixture was cooled on ice and treated dropwise (during 5 min) with 1 M lithium bis(trimethylsilyl)amide (1.5 mL, 1.5 mmol). After 1.5 h at 0 °C the reaction was quenched with saturated NH_4Cl (5 mL). The organic products were extracted with EtOAc (2 × 10 mL) and the combined organic phases washed with saturated NaCl (10 mL). The organic phase was dried over Na_2SO_4, evaporated in vacuo, and purified by flash chromatography using a gradient of EtOAc in heptane as eluent. The title compound **3** was obtained as a white solid. UPLC−MS (ESI+) *m*/*z* 326.03 (MH$^+$). ^{1}H NMR (300 MHz, DMSO-d_6) δ 8.66 (s, 2H), 7.85 (dd, *J* = 8.5, 2.0 Hz, 1H), 7.55 (d, *J* = 2.0 Hz, 1H), 7.14 (d, *J* = 8.5 Hz, 1H), 4.78 (s, 2H), 3.88 (s, 3H), 3.85 (s, 3H). ^{13}C NMR (75 MHz, DMSO) δ 191.90, 153.68, 148.67, 147.08, 141.59, 132.81, 128.41, 123.08, 111.00, 110.31, 55.79, 55.52, 40.50. Yield 120 mg (73%).

2-(3,5-Dichloropyridin-4-yl)-1-(2,3,4-trimethoxyphenyl)-ethanone (4). Methyl 2,3,4-trimethoxybenzoate (2.7 g, 10 mmol) and 3,5-dichloro-4-methylpyridine dissolved in dry THF (40 mL). The mixture was cooled on ice and treated dropwise (during 5 min) with 1 M lithium bis(trimethylsilyl)amide (12 mL, 12 mmol). After 1.5 h at 0 °C the reaction was quenched with saturated NH_4Cl (100 mL). The organic products were extracted with EtOAc (2 × 100 mL) and the combined organic phases washed with saturated NaCl (100 mL). The organic phase was dried over Na_2SO_4, evaporated in vacuo, and purified by flash chromatography using a gradient of EtOAc in heptane as eluent. The title compound **4** was obtained as a white solid. UPLC−MS (ESI+) *m*/*z* 356.05 (MH$^+$). ^{1}H NMR (600 MHz, DMSO-d_6) δ 8.66 (s, 2H), 7.52 (d, *J* = 8.9 Hz, 1H), 6.98 (d, *J* = 8.9 Hz, 1H), 4.66 (s, 2H), 4.00 (s, 3H), 3.89 (s, 3H), 3.81 (s, 3H). ^{13}C NMR (151 MHz, DMSO) δ 192.37, 157.83, 153.70, 147.03, 141.59, 141.49, 132.76, 125.29, 123.54, 107.99, 61.45, 60.40, 56.13, 44.38.

2-(3,5-Dichloro-pyridin-4-yl)-1-(2-hydroxy-3,4-dimethoxy-phenyl)-ethanone (4a). To a solution of **4** (20 g, 56 mmol) in DCM (75 mL) was slowly added 1 M BCl_3 (95 mL, 95 mmol) in DCM. The reaction mixture was stirred under nitrogen at room temperature for 2 h. Water (50 mL) was added slowly followed by EtOH (200 mL). The white precipitate was filtered and recrystallized from EtOH. The title compound **4a** was obtained as a white solid. ^{1}H NMR (300 MHz, $CDCl_3$) δ 11.92 (1H, s), 8.54 (2H, s), 7.68 (1H, d), 6.60 (1H, d), 4.67 (2H, s), 3.98 (3H, s), 3.90 (3H, s). Yield 14.2 g (74%)

2-(3,5-Dichloropyridin-4-yl)-1-(2,3-dihydroxy-4-methoxyphenyl)ethanone (4b). To a solution of **4** (1.25g, 3.5 mmol) in AcOH (100%, 9.25 mL) was added HI (55−58%, 4.55 mL), and the reaction mixture was heated to 80 °C for 18 h. The reaction mixture was cooled to room temperature and evaporated in vacuo. $NaHCO_3$ (saturated, 150 mL) was added slowly, followed by NaCl (saturated, 50 mL). The organic products were extracted with EtOAc (4 × 100 mL). The combined organic phases were washed with saturated NaCl (2 × 100 mL) and 10% $Na_2S_2O_3$ (100 mL) and dried over Na_2SO_4 and evaporated in vacuo. The title compound **4b** was obtained as a brown solid. ^{1}H NMR (300 MHz, $CDCl_3$) δ 11.88 (1H, s), 8.54 (2H, s), 7.51 (1H, d), 6.60 (1H, d), 5.62 (1H, bs), 4.67 (2H, s), 4.00 (3H, s). Yield 0.935g (81%)

2-(3,5-Dichloropyridin-4-yl)-1-(2,4-dimethoxy-3-hydroxyphenyl)ethanone (4c). To a solution of **4b** (0.77 mmol) in dry DMF (5.5 mL) was added K_2CO_3 (0.77 mmol) followed by methyl iodide (0.77 mmol). The reaction mixture was stirred at room temperature for 18 h. NH_4Cl (saturated, 15 mL) was added, and the organic products were extracted with EtOAc (3 × 15 mL). The combined organic phases were washed with saturated NaCl (2 × 15 mL). The organic phase was dried over Na_2SO_4, evaporated in vacuo, and purified by flash chromatography using a gradient of EtOAc in toluene as eluent. The title compound **4c** was obtained as a yellow solid. ^{1}H NMR (600 MHz, $CDCl_3$) δ 8.50 (s, 2H), 7.43 (d, *J* = 8.8 Hz, 1H), 6.75 (d, *J* = 8.8 Hz, 1H), 5.73 (s, 1H), 4.70 (s, 2H), 4.08 (s, 3H), 3.98 (s, 3H). Yield 72 mg (27%).

General Protocol for Preparation of Compound 5, 6, and 7. To a solution of **4c** (0.06 mmol) in dry diethyl ketone (0.6 mL) was added K_2CO_3 (0.06 mmol) followed by catalytic amounts of KI (2 mg, 0.012 mmol) and an alkyl halide (0.06 mmol). The reaction mixture was stirred at 80 °C for 24 h. The reaction mixture was cooled to room temperature and evaporated in vacuo. The reaction mixture was redissolved in EtOAc (5 mL) and washed with saturated NaCl (2 × 5 mL). The organic phase was dried over Na_2SO_4 and evaporated in vacuo. The pure compounds were obtained by standard preparative HPLC purification.

dx.doi.org/10.1021/jm500378a | J. Med. Chem. XXXX, XXX, XXX−XXX

1-(3-Ethoxy-2,4-dimethoxy-phenyl)-2-(3,5-dichloro-pyridin-4-yl)-ethanone Compound (5). UPLC−MS (ESI+) m/z 370.06 (MH^+). ^1H NMR (300 MHz, $CDCl_3$) δ 8.50 (s, 2H), 7.61 (d, J = 8.9 Hz, 1H), 6.76 (d, J = 8.9 Hz, 1H), 4.68 (s, 2H), 4.11 (q, J = 7.0 Hz, 2H), 1.43 (t, J = 7.0 Hz, 3H). ^{13}C NMR (75 MHz, $CDCl_3$) δ 192.68, 158.45, 154.75, 147.19, 141.71, 141.05, 133.55, 125.99, 124.39, 107.35, 69.32, 61.49, 56.18, 44.93, 15.66. Alkyl halide: ethyl iodide.

1-(3-Cyclopropylmethoxy-2,4-dimethoxyphenyl)-2-(3,5-dichloropyridin-4-yl)ethanone (6). UPLC−MS (ESI+) m/z 396.08 (MH^+). ^1H NMR (300 MHz, $CDCl_3$) δ 8.50 (s, 2H), 7.61 (d, J = 8.9 Hz, 1H), 6.75 (d, J = 8.9 Hz, 1H), 4.68 (s, 2H), 4.12 (s, 3H), 3.92 (s, 3H), 3.85 (d, J = 7.2 Hz, 2H), 1.42−1.18 (m, 1H), 0.72−0.53 (m, 2H), 0.42−0.24 (m, 2H). ^{13}C NMR (75 MHz, $CDCl_3$) δ 192.68, 158.45, 154.80, 147.20, 141.69, 141.11, 133.54, 126.02, 124.32, 107.32, 78.49, 61.58, 56.17, 44.92, 11.01, 3.18. Alkyl halide: 1-bromomethyl-cyclopropane.

1-(3-Cyclopentoxy-2,4-dimethoxyphenyl)-2-(3,5-dichloro-pyridin-4-yl)ethanone (7). UPLC−MS (ESI+) m/z 410.10 (MH^+). ^1H NMR (300 MHz, $CDCl_3$) δ 8.50 (s, 2H), 7.60 (d, J = 8.9 Hz, 1H), 6.76 (d, J = 8.9 Hz, 1H), 4.97−4.76 (m, 1H), 4.69 (s, 2H), 4.05 (s, 3H), 3.91 (s, 3H), 2.06−1.82 (m, 4H), 1.83−1.55 (m, 4H). ^{13}C NMR (75 MHz, $CDCl_3$) δ 192.83, 158.68, 155.10, 147.19, 141.73, 140.17, 133.56, 125.78, 124.53, 107.42, 85.25, 61.18, 56.12, 44.94, 32.86, 23.63. Alkyl halide: cyclopentyl bromide.

General Protocol for Preparation of Compound 8, 9, 10, 11 and 22. To a solution of **4a** (0.035 mmol) in dry DMSO (0.25 mL) was added 2 M K_2CO_3 (25 μL, 0.050 mmol) followed by an alkyl halide (0.053 mmol) dissolved in DMSO (25 μL). The reaction mixture was left at room temperature for 48 h and then filtered. The pure compounds were obtained by standard preparative HPLC purification.

1-(2-Benzyloxy-3,4-dimethoxyphenyl)-2-(3,5-dichloropyridin-4-yl)ethanone (8). UPLC−MS (ESI+) m/z 432.07 (MH^+). ^1H NMR (600 MHz, $CDCl_3$) δ 8.45 (s, 2H), 7.62 (d, J = 8.9 Hz, 1H), 7.51−7.47 (m, 2H), 7.41−7.37 (m, 2H), 7.37−7.33 (m, 1H), 6.79 (d, J = 8.9 Hz, 1H), 5.28 (s, 2H), 4.57 (s, 2H), 3.96 (s, 3H), 3.94 (s, 3H). ^{13}C NMR (151 MHz, $CDCl_3$) δ 192.88, 158.12, 153.17, 147.12, 142.05, 141.62, 136.64, 133.46, 128.74, 128.61, 128.53, 126.10, 125.18, 107.48, 76.62, 61.13, 56.23, 45.28. Alkyl halide: benzyl chloride.

2-(3,5-Dichloropyridin-4-yl)-1-(3,4-dimethoxy-2-phenethyloxyphenyl)ethanone (9). UPLC−MS (ESI+) m/z 446.09 (MH^+). ^1H NMR (600 MHz, DMSO-d_6) δ 8.63 (s, 2H), 7.52 (d, J = 8.9 Hz, 1H), 7.36−7.31 (m, 2H), 7.26−7.21 (m, 2H), 7.11−7.05 (m, 1H), 6.97 (d, J = 8.9 Hz, 1H), 4.43 (t, J = 6.6 Hz, 2H), 4.40 (s, 2H), 3.88 (s, 3H), 3.69 (s, 3H), 3.13 (t, J = 6.6 Hz, 2H). ^{13}C NMR (151 MHz, $CDCl_3$) δ 192.50, 158.13, 153.32, 147.12, 142.12, 141.70, 138.06, 133.43, 129.08, 128.48, 126.52, 126.23, 124.57, 107.37, 74.92, 60.96, 56.18, 44.95, 36.98. Alkyl halide: 1-bromo-2-phenyl-ethane.

2-(3,5-Dichloropyridin-4-yl)-1-[3,4-dimethoxy-2-(3-phenylpropoxy)phenyl]ethanone (10). UPLC−MS (ESI+) m/z 460.11 (MH^+). ^1H NMR (600 MHz, $CDCl_3$) δ 8.50 (s, 2H), 7.60 (d, J = 8.9 Hz, 1H), 7.29−7.25 (m, 2H), 7.24−7.20 (m, 2H), 7.20−7.16 (m, 1H), 6.75 (d, J = 8.9 Hz, 1H), 4.69 (s, 2H), 4.28 (t, J = 6.7 Hz, 2H), 3.93 (s, 3H), 3.88 (s, 3H), 2.85 (dd, J = 8.7, 6.7 Hz, 2H), 2.28−2.16 (m, 2H). ^{13}C NMR (151 MHz, $CDCl_3$) δ 192.81, 158.08, 153.49, 147.20, 142.02, 141.57, 141.31, 133.51, 128.47, 128.36, 126.08, 126.05, 124.91, 107.23, 74.28, 61.03, 56.17, 45.07, 32.30, 32.00. Alkyl halide: 1-bromo-3-phenylpropane.

2-(3,5-Dichloro-4-pyridyl)-1-[2-[2-(4-hydroxyphenyl)-ethoxy]-3,4-dimethoxyphenyl]ethanone (11). UPLC−MS (ESI+) m/z 462.09 (MH^+). ^1H NMR (300 MHz, DMSO-d_6) δ 9.06 (s, 1H), 8.62 (s, 2H), 7.51 (d, J = 9.0 Hz, 1H), 7.17−7.04 (m, 2H), 6.95 (d, J = 9.0 Hz, 1H), 6.66−6.52 (m, 2H), 4.40 (s, 2H), 4.36 (t, J = 6.7 Hz, 2H), 3.88 (s, 3H), 3.72 (s, 3H), 3.01 (t, J = 6.7 Hz, 2H). ^{13}C NMR (151 MHz, DMSO) δ 192.18, 157.87, 155.74, 152.63, 146.92, 141.55, 141.49, 132.60, 129.70, 127.97, 125.43, 123.51, 114.93, 107.91, 74.74, 60.38, 56.09, 44.46, 35.14. Alkyl halide: 1-bromo-3-(4-hydroxyphenyl)-propane. NaH was used in place of K_2CO_3 and heating to 60 °C overnight was applied to obtain the desired product.

2-{6-[2-(3,5-Dichloropyridin-4-yl)acetyl]-2,3-dimethoxyphenoxy}acetamide (22). UPLC−MS (ESI+) m/z 399.06 (MH^+). ^1H NMR (300 MHz, DMSO-d_6) δ 8.65 (s, 2H), 7.66 (s, 1H), 7.61 (d, J = 8.9 Hz, 1H), 7.39 (s, 1H), 6.99 (d, J = 8.9 Hz, 1H), 4.80 (s, 2H), 4.63 (s, 2H), 3.92 (s, 3H), 3.81 (s, 3H). Alkyl halide: 2-chloroacetamide.

4-[2-[6-[2-(3,5-Dichloro-4-pyridyl)acetyl]-2,3-dimethoxyphenoxy]ethyl]benzoic Acid (13). To a solution of **4a** (0.87 g, 2.5 mmol) in dry THF (25 mL) was added methyl 4-(2-hydroxyethyl)benzoate (0.37 g, 2 mmol) followed by solid phase bound triphenylphosphine (2 g with a loading of 1.48 mmol/g, 3 mmol). The reaction mixture was cooled to 0 °C, and DEAD (0.93 mL, 3 mmol) was added. The reaction mixture was gently vortexed at room temperature for 24 h. The reaction mixture was filtered and the solvent evaporated in vacuo. The organic products were redissolved in EtOAc (50 mL) and washed with 2 N NaOH (4 × 50 mL) and saturated NaCl (50 mL). The organic phase was dried over Na_2SO_4 and evaporated in vacuo to provide methyl 4-[2-[6-[2-(3,5-dichloro-4-pyridyl)acetyl]-2,3-dimethoxyphenoxy]ethyl]benzoate as a white solid. Yield 535 mg (52%). The compound (1 mmol) was dissolved in THF (10 mL). MeOH (5 mL) was added followed by LiOH (0.22 g, 5 mmol) dissolved in water (5 mL). The reaction mixture was heated to 50 °C for 4 h and then cooled to room temperature. The reaction mixture was acidified to pH 1 by addition of 2 N HCl (7 mL). The white precipitate was filtered and washed with water (3 × 10 mL). The precipitate was dried in vacuo to provide the title compound **13** as a white solid. UPLC−MS (ESI+) m/z 490.08 (MH^+). ^1H NMR (300 MHz, DMSO-d_6) δ 12.69 (s, 1H), 8.58 (s, 2H), 7.85−7.74 (m, 2H), 7.52 (d, J = 8.9 Hz, 1H), 7.50−7.41 (m, 2H), 6.96 (d, J = 8.9 Hz, 1H), 4.47 (t, J = 6.2 Hz, 2H), 4.23 (s, 2H), 3.88 (s, 3H), 3.71 (s, 3H), 3.21 (t, J = 6.2 Hz, 2H). Yield 254 mg (49%).

{6-[2-(3,5-Dichloropyridin-4-yl)acetyl]-2,3-dimethoxyphenoxy}acetic Acid (14). To a solution of **4a** (1.37 g, 4.1 mmol) in dry NMP (20 mL) was added ethyl bromoacetate (660 μL, 6.1 mmol) followed by K_2CO_3 (830 mg, 6.1 mmol). The reaction mixture was stirred at room temperature overnight. Water (100 mL) was added, and the organic products were extracted with EtOAc (2 × 100 mL). The combined organic phases were washed with water (100 mL), brine (100 mL) and dried over $MgSO_4$. The solvent were removed in vacuo and the pure product was obtained be standard silica gel chromatography to provide {6-[2-(3,5-dichloropyridin-4-yl)-acetyl]-2,3-dimethoxyphenoxy}acetic acid ethyl ester as a white solid. Yield 990 mg (78%). The compound was redissolved in MeOH−water (1:1, 50 mL) by heating. LiOH (490 mg, 12 mmol, 5 equiv) was added, and the reaction mixture was stirred at room temperature for 1 h. The reaction mixture was acidified to pH 1 by addition of 1 N HCl (15 mL) and extracted with EtOAc (2 × 100 mL). The combined organic phases were washed with brine (100 mL) and dried over $MgSO_4$. The solvent was removed in vacuo to provide the title compound **14** as a white solid. UPLC−MS (ESI+) m/z 489.10 (MH^+). ^1H NMR (300 MHz, DMSO-d_6) δ 8.63 (s, 2H), 7.49 (d, J = 9.0 Hz, 1H), 6.95 (d, J = 9.0 Hz, 1H), 4.90 (s, 2H), 4.83 (s, 2H), 3.89 (s, 3H), 3.78 (s, 3H). ^{13}C NMR (151 MHz, $CDCl_3$) δ 191.92, 168.54, 158.21, 152.17, 147.24, 141.79, 140.81, 137.93, 133.41, 128.50, 127.87, 127.33, 126.43, 122.84, 107.04, 73.10, 61.07, 56.27, 43.18, 43.09. Yield 0.85g (92%).

General Protocol for Preparing Compounds 12, 15, 16, 17, 18, 19, and 20. To a solution of a carboxylic acid (**13** or **14**, 0.05 mmol) in dry DMF (0.2 mL) was added an amine (0.15 mmol dissolved in DMF (50 μL) followed by DIPEA (0.15 mmol) and HATU (0.075 mmol) dissolved in DMF (50 μL). The reaction mixture was stirred at room temperature for 48 h. The pure compounds were obtained by standard preparative HPLC purification.

4-[2-[6-[2-(3,5-Dichloro-4-pyridyl)acetyl]-2,3-dimethoxyphenoxy]ethyl]-*N*-methylbenzamide (12). UPLC−MS (ESI+) m/z 503.11 (MH^+). ^1H NMR (300 MHz, $CDCl_3$) δ 8.47 (s, 2H), 7.71−7.63 (m, 2H), 7.61 (d, J = 8.9 Hz, 1H), 7.42−7.31 (m, 2H), 6.75 (d, J = 8.9 Hz, 1H), 6.11 (q, J = 4.8 Hz, 1H), 4.48 (t, J = 6.6 Hz, 2H), 4.41 (s, 2H), 3.92 (s, 3H), 3.75 (s, 3H), 3.21 (t, J = 6.6

dx.doi.org/10.1021/jm500378a | J. Med. Chem. XXXX, XXX, XXX−XXX

Hz, 2H), 2.96 (d, J = 4.8 Hz, 3H). Carboxylic acid: **13**. Amine: methylamine hydrochloride.

***N*-Benzyl-2-{6-[2-(3,5-dichloropyridin-4-yl)acetyl]-2,3-dimethoxyphenoxy}acetamide (15).** UPLC−MS (ESI+) m/z 400.03 (MH^+). ^{1}H NMR (400 MHz, DMSO-d_6) δ 8.74 (t, J = 6.1 Hz, 1H), 8.64 (s, 2H), 7.61 (d, J = 8.9 Hz, 1H), 7.36−7.14 (m, 5H), 7.00 (d, J = 8.9 Hz, 1H), 4.76 (s, 2H), 4.73 (s, 2H), 4.35 (d, J = 6.1 Hz, 2H), 3.90 (s, 3H), 3.77 (s, 3H). Carboxylic acid: **14**. Amine: benzylamine.

2-{6-[2-(3,5-Dichloropyridin-4-yl)acetyl]-2,3-dimethoxyphenoxy}-*N*-phenylacetamide (16). UPLC−MS (ESI+) m/z 475.07 (MH^+). ^{1}H NMR (300 MHz, $CDCl_3$) δ 9.96 (s, 1H), 8.51 (s, 2H), 7.74 (d, J = 8.9 Hz, 1H), 7.64−7.50 (m, 2H), 7.34−7.18 (m, 2H), 7.14−7.00 (m, 1H), 6.81 (d, J = 8.9 Hz, 1H), 4.80 (s, 2H), 4.65 (s, 2H), 3.99 (s, 3H), 3.89 (s, 3H). ^{13}C NMR (75 MHz, $CDCl_3$) δ 192.74, 166.91, 158.56, 152.63, 147.30, 141.76, 140.90, 138.00, 133.50, 128.78, 126.69, 124.07, 122.28, 119.53, 106.83, 73.48, 61.10, 56.34, 42.80. Carboxylic acid: **14**. Amine: aniline.

2-{6-[2-(3,5-Dichloropyridin-4-yl)acetyl]-2,3-dimethoxyphenoxy}-*N*-methyl-*N*-phenylacetamide (17). UPLC−MS (ESI+) m/z 489.09 (MH^+). ^{1}H NMR (300 MHz, $CDCl_3$) δ 8.48 (s, 2H), 7.59 (d, J = 8.9 Hz, 1H), 7.48−7.39 (m, 2H), 7.38−7.31 (m, 1H), 7.25−7.19 (m, 2H), 6.71 (d, J = 8.9 Hz, 1H), 4.83 (s, 2H), 4.69 (s, 2H), 3.90 (s, 3H), 3.77 (s, 3H), 3.31 (s, 3H). ^{13}C NMR (75 MHz, $CDCl_3$) δ 193.06, 167.35, 157.86, 152.46, 147.14, 142.12, 142.06, 141.15, 133.66, 130.14, 128.54, 127.17, 126.29, 124.58, 107.21, 70.67, 61.16, 56.15, 45.41, 37.42. Carboxylic acid: **14**. Amine: *N*-methylaniline.

2-{6-[2-(3,5-Dichloropyridin-4-yl)acetyl]-2,3-dimethoxyphenoxy}-*N*-(2-hydroxyethyl)acetamide (18). UPLC−MS (ESI+) m/z 443.08 (MH^+). ^{1}H NMR (600 MHz, DMSO-d_6) δ 8.64 (s, 2H), 8.14 (t, J = 6.0 Hz, 1H), 7.59 (d, J = 8.9 Hz, 1H), 6.99 (d, J = 8.9 Hz, 1H), 4.77 (s, 2H), 4.65 (s, 2H), 3.90 (s, 3H), 3.79 (s, 3H), 3.41 (t, J = 6.0 Hz, 3H), 3.20 (q, J = 6.0 Hz, 2H). ^{13}C NMR (151 MHz, $CDCl_3$) δ 192.90, 169.85, 158.51, 152.42, 147.38, 141.82, 140.63, 133.37, 126.73, 122.43, 106.96, 73.09, 62.39, 61.14, 56.32, 43.05, 42.35. Carboxylic acid: **14**. Amine: 2-hydroxyethylamine.

2-{6-[2-(3,5-Dichloropyridin-4-yl)acetyl]-2,3-dimethoxyphenoxy}-*N*-(2-methoxyethyl)acetamide (19). UPLC−MS (ESI+) m/z 457.09 (MH^+). ^{1}H NMR (600 MHz, DMSO-d_6) δ 8.65 (s, 2H), 8.23 (t, J = 5.6 Hz, 1H), 7.61 (d, J = 8.9 Hz, 1H), 6.99 (d, J = 8.9 Hz, 1H), 4.77 (s, 2H), 4.65 (s, 2H), 3.91 (s, 3H), 3.79 (s, 3H), 3.35 (t, J = 5.6 Hz, 2H), 3.29 (q, J = 5.6 Hz, 2H), 3.16 (s, 3H). ^{13}C NMR (151 MHz, $CDCl_3$) δ 191.97, 168.72, 158.17, 152.13, 147.24, 141.82, 141.02, 133.54, 126.37, 123.22, 107.25, 73.05, 70.87, 61.14, 58.56, 56.27, 43.52, 38.82. Carboxylic acid: **14**. Amine: 2-methoxyethylamine.

2-{6-[2-(3,5-Dichloropyridin-4-yl)acetyl]-2,3-dimethoxyphenoxy}-*N*-propylacetamide (20). UPLC−MS (ESI+) m/z 441.09 (MH^+). ^{1}H NMR (600 MHz, $CDCl_3$) δ 8.52 (s, 2H), 7.87−7.76 (m, 1H), 7.68 (d, J = 8.9 Hz, 1H), 6.79 (d, J = 8.9 Hz, 1H), 4.67 (s, 2H), 4.60 (s, 2H), 3.97 (s, 3H), 3.87 (s, 3H), 3.35−3.21 (m, 2H), 1.50 (h, J = 7.3 Hz, 2H), 0.87 (t, J = 7.3 Hz, 3H). ^{13}C NMR (151 MHz, $CDCl_3$) δ 192.13, 168.59, 158.24, 152.33, 147.25, 141.80, 140.93, 133.46, 126.40, 122.88, 106.92, 73.16, 61.08, 56.28, 43.15, 40.79, 22.50, 11.37. Carboxylic acid: **14**. Amine: propylamine.

***N*-Benzyl-2-{6-[2-(3,5-dichloro-1-oxypyridin-4-yl)acetyl]-2,3-dimethoxyphenoxy}acetamide (21).** To a solution of **15** (10 mg, 0.021 mmol) in dry DCM (0.25 mL) was added methyltrioxorhenium (26 mg, 0.105 mmol) followed by 30% hydrogen peroxide (6.4 μL, 0.063 mmol). The reaction mixture was stirred at room temperature overnight. MnO_2 (5.5 mg, 0.063 mmol) was added, and after 2 min the reaction mixture was filtered and the solvent evaporated in vacuo. The title compound **21** was obtained by standard preparative HPLC purification. UPLC−MS (ESI+) m/z 505.09 (MH^+). ^{1}H NMR (300 MHz, $CDCl_3$) δ 8.15 (2H, s), 8.10 (1H, bs), 7.62 (1H, d), 7.30 (5H, m), 6.76 (1H, d), 4.72 (2H, s), 4.50 (2H, d), 4.46 (2H, s), 3.95 (3H, s), 3.80 (3H, s). ^{13}C NMR (75 MHz, $CDCl_3$) δ 191.57, 168.50, 158.44, 152.25, 141.81, 137.90, 137.45, 134.13, 131.63, 128.52, 127.97, 127.41, 126.43, 122.48, 107.13, 73.11, 61.09, 56.30, 43.21, 42.32.

Crystallography. The crystal structures of the ethylisoxazole analogue of piclamilast and **15** complexed with PDE4D were solved at ActiveSight, San Diego, CA, U.S., with their off-the-shelf protein structure determination service. The structures were solved to a resolution of 2.2 and 2.5 Å, respectively, using a PDE4D construct with residues 153−512 (1XM4 residue numbering).

Hydrogens were added, H-bonds were optimized, and the complex was minimized using the protein preparation wizard implemented in Maestro.

Modeling. The dihedral coordinate scans of **1**, **2**, and **4** (enol form) were done with MacroModel (OPLS-2005, water, TNCG minimization) using 5° increments. The QM energies of **1**−**4** listed in Table 1 were obtained by taking the local minimum conformation from the coordinate scan (see Figure 3B) with the dihedral closest to that observed for piclamilast in the 1XM4 structure (144.5°). Subsequently, a QM minimization was performed with Jaguar. DFT was used with default settings (B3LYP, 6-31**). Solvent was set to Water (PBF model). Finally, the QM energy of the minimized conformation was estimated using DFT settings B3LYP-MM, cc-pVDZ^{+2}, SM8 solvent model. A similar procedure was performed for the global minimum conformation from the coordinate scan, and the relative QM energy of the bioactive conformation was taken as the difference.

Docking of the enol form of **9** to PDE4 was performed using the PDE4−piclamilast ethylisoxazole analogue crystal structure (Figure 4A). Compound **9** was docked flexibly with Glide XP with 0.8 scaling of the protein atoms and default settings for ligand scaling. The highest scoring docking pose is shown in Figure 4B.

MacroModel, Jaguar, Glide, and Maestro were used as implemented in the 2013-2 software suite; Schrödinger, LLC, New York, NY, 2013.

PDE4 Assay. Human recombinant PDE4D (Genbank accession no. NM_006203) was incubated for 1 h with the test compound at concentrations up to 10 μM, with cAMP (1×10^{-5} M) and with a low amount (0.021 MBq) of radioactively labeled cAMP. At the end of the incubation, the cleavage of the substrate was evaluated by the binding of the AMP product to SPA beads, which generate chemoluminescence when bound to the radioactive tracer. The AMP product inhibited the binding of the radioactive tracer to the beads, and the luminescent signal was competed.

The results were calculated as the molar concentrations resulting in 50% inhibition of the substrate cleavage compared to controls samples and are expressed as a range of IC_{50} (nM).

TNF-α Release. Human peripheral blood mononuclear cells (PBMCs) were isolated from buffy coats. The blood is mixed with saline at a ratio of 1:1, and the PBMCs were isolated using Lymphoprep tubes (Nycomed, Norway). The PBMCs were suspended in RPMI 1640 with 0.5% human serum albumin, pen/strep, and 2 mM L-glutamine at a concentration of 5×10^5 cells/mL.

The cells were preincubated for 30 min with the test compounds in 96-well tissue culture plates and stimulated for 18 h with lipopolysaccharide 1 mg/mL (Sigma). TNF-α concentration in the supernatants was measured using homogeneous time-resolved fluorescence resonance (TR-FRET). The assay is quantified by measuring fluorescence at 665 nm (proportional to TNF-a concentration) and 620 nm (control). Results are expressed as IC_{50} values calculated from inhibition curves using as positive controls the secretion in LPS stimulated wells and as negative controls the secretion in unstimulated cells.

HLM (Human Liver Microsomes) Assay. Incubations of test compounds in DMSO, diluted with phosphate buffer, pH 7.4, at 0.5 μM were carried out with human liver microsomes (0.5 mg/mL). The percentage of organic solvent in the incubations was 1%. The human liver microsomal suspension in phosphate buffer was mixed with NADPH (1 mM) and preheated to 37 °C before test compound was added. Aliquots were taken at 0, 5, 10, 20, and 30 min, and reactions were terminated by addition of methanol containing analytical internal standard (IS).

The results were expressed as apparent clearance (Cl_{app}) (mL min^{-1} kg^{-1}) and hepatic extraction ratio (E_h) (%) calculated from the rate constant (k) (min^{-1}) of test compound depletion. The upper limit for determination of Cl_{app} is 200 mL min^{-1} kg^{-1} (corresponding to

dx.doi.org/10.1021/jm500378a | J. Med. Chem. XXXX, XXX, XXX−XXX

extraction ratio of 91%), and the lower limit is 10 mL min^{-1} kg^{-1} (corresponding to extraction ratio of 33%).

Emesis Study. Domestic ferret (*Mustela putorius furo*), 24 weeks, 1.0−1.3 kg were dosed iv with compound dissolved 2-hydroxypropyl-β-cyclodextrin in sterile water (volume 5 mL/kg). After treatment, animals were singly housed (polycarbonate type E, Charles River Laboratories; 405 mm × 255 mm × 197 mm) and emetic episodes and associated prodromic signs were counted for 2 h. Emesis parameters were the following: number of ferrets showing retches and vomits; latency to first retching (hh:mm); latency to first vomiting (hh:mm); retching (number of retches); vomiting (number of vomits). Prodromic signs were the following: licking; mouth scratching; yawning; wet dog shakes and backward walking.

AUTHOR INFORMATION

Corresponding Author

*E-mail: simon.nielsen@leo-pharma.com. Phone: +45 72263703.

Present Addresses

[†]T.D.P.: DTU Admission Course, Lautrupvang 15, DK-2750 Ballerup, Denmark.

[‡]C.A.: Novo Nordisk A/S, Immunopharmacology 479, Novo Nordisk Park, DK-2760 Måløv, Denmark.

[§]A.M.V.: Division of Toxicology and Risk Assessment, National Food Institute, Technical University of Denmark, Mørkhøj Bygade 19, DK-2860 Søborg, Denmark.

Notes

The authors declare no competing financial interest.

ACKNOWLEDGMENTS

We thank all the dedicated PDE4 people at LEO for making the selection of LEO 29102 a reality.

REFERENCES

(1) Hanifin, J. M.; Reed, M. L. A population-based survey of eczema prevalence in the United States. *Dermatitis* **2007**, *18*, 82−91.

(2) Watson, W.; Kapur, S. Atopic dermatitis. *J. Allergy Clin. Immunol.* **2011**, *7* (Suppl. 1), S4.

(3) Lewis-Jones, S. Quality of life and childhood atopic dermatitis: the misery of living with childhood eczema. *Int. J. Clin. Pract.* **2006**, *60*, 984−992.

(4) Zheng, T.; Yu, J.; Oh, M. H.; Zhu, Z. The atopic march: progression from atopic dermatitis to allergic rhinitis and asthma. *J. Allergy Clin. Immunol.* **2011**, *3*, 67−73.

(5) Thaci, D.; Salgo, R. Malignancy concerns of topical calcineurin inhibitors for atopic dermatitis: facts and controversies. *Clin. Dermatol.* **2010**, *28*, 52−56.

(6) Bender, A. T.; Beavo, J. A. Cyclic nucleotide phosphodiesterases: molecular regulation to clinical use. *Pharmacol. Rev.* **2006**, *58*, 488−520.

(7) Kodimuthali, A.; Jabaris, S. S. L.; Pal, M. Cyclic nucleotide phosphodiesterases: molecular regulation to clinical use. *J. Med. Chem.* **2008**, *51*, 5471−5489.

(8) Giembycz, M. A. Can the anti-inflammatory potential of PDE4 inhibitors be realized: guarded optimism or wishful thinking? *Br. J. Pharmacol.* **2008**, *155*, 288−290.

(9) Ashton, M. J.; Cook, D. C.; Fenton, G.; Karlsson, J.-A.; Palfreyman, M. N.; Raeburn, D.; Ratcliffe, A. J.; Souness, J. E.; Thurairatnam, S.; Vicker, N. Selective type IV phosphodiesterase inhibitors as antiasthmatic agents. The syntheses and biological activities of 3-(cyclopentyloxy)-4-methoxybenzamides and analogues. *J. Med. Chem.* **1994**, *37*, 1696−1703.

(10) Card, G. L.; England, B. P.; Suzuki, Y.; Fong, D.; Powell, B.; Lee, B.; Luu, C.; Tabrizizad, M.; Gillette, S.; Ibrahim, P. N.; Artis, D. R.; Bollag, G.; Milburn, M. V.; Kim, S.-H.; Schlessinger, J.; Zhang, K. Y. J. Structural basis for the activity of drugs that inhibit phosphodiesterases. *Structure* **2004**, *12*, 2233−2247.

(11) Ricerca Biosciences LLC (formerly MDS Pharma Services). http://www.ricerca.com/.

(12) GreenScreen HC. http://www.gentronix.co.uk/product/greenscreen/.

(13) Griffiths, C. E.; Van Leent, E. J.; Gilbert, M.; Traulsen, J.; Cipamyflline Study Group.. Randomized comparison of the type 4 phosphodiesterase inhibitor cipamfylline cream, cream vehicle and hydrocortisone 17-butyrate cream for the treatment of atopic dermatitis. *Br J. Dermatol.* **2002**, *147*, 299−307.

(14) LEO 29102 Single and Multiple Dose Study by Dermal Application, NCT00891709. http://www.ClinicalTrials.gov.

(15) LEO 29102 Cream in the Treatment of Atopic Dermatitis, NCT01037881. http://www.ClinicalTrials.gov.

(16) Felding, J.; Nielsen, S. F.. Substituted Acetophenones Useful as PDE4 Inhibitors. U.S. Patents US 8,148,537 B2 and US 8,324,394 B2, 2012.

(17) R&D Insight Database. http://www.adis.com.